Volume 313, number 1, 85–89 FEBS 11706 November 1992

Osteoclasts express high levels of p60$^{c\text{-}src}$, preferentially on ruffled border membranes

Sakae Tanaka[a,c], Naoyuki Takahashi[a], Nobuyuki Udagawa[a], Takahisa Sasaki[a], Yasuhisa Fukui[b], Takahide Kurokawa[c] and Tatsuo Suda[a]

[a]*Departments of Biochemistry and Oral Anatomy, School of Dentistry, Showa University, 1-5-8 Hatanodai, Shinagawa-ku, Tokyo 142, Japan,* [b]*Laboratory of Biochemistry, Department of Agricultural Chemistry, University of Tokyo, 1-1-1 Yayoi, Bunkyo-ku, Tokyo 113, Japan* and [c]*Department of Orthopedic Surgery, School of Medicine, University of Tokyo, 7-3-1 Hongo, Bunkyo-ku, Tokyo 113, Japan*

Received 26 August 1992; revised version received 17 September 1992

Expression of p60$^{c\text{-}src}$, the normal cellular counterpart of the transforming protein of Rous sarcoma virus (RSV), p60$^{v\text{-}src}$, was examined in mouse and rat authentic osteoclasts and mouse osteoclast-like multinucleated cells (MNCs) formed in vitro. In co-cultures of mouse osteoblastic cells and spleen cells, the expression of p60$^{c\text{-}src}$ strikingly increased on day 5 in parallel with the appearance of MNCs in the presence of 1α,25-dihydroxyvitamin D_3 (1α,25$(OH)_2D_3$). Immunohistochemical examination confirmed the high level expression of p60$^{c\text{-}src}$ in both mouse authentic osteoclasts and MNCs. Electron microscopic examination revealed that p60$^{c\text{-}src}$ was primarily localized on ruffled border membranes and vacuoles, but not on the clear zone in rat authentic osteoclasts. These results suggest that p60$^{c\text{-}src}$ is important in osteoclastic bone resorption.

Osteoclast; p60$^{c\text{-}src}$; Tyrosine kinase; 1α,25-dihydroxyvitamin D_3; Osteopetrosis

1. INTRODUCTION

p60$^{c\text{-}src}$ is the normal cellular counterpart of the transforming protein of Rous sarcoma virus (RSV), p60$^{v\text{-}src}$. p60$^{c\text{-}src}$ is a protein–tyrosine kinase which is associated with the cytoplasmic face of the cellular membrane (see [1,2]). It has been reported that terminally differentiated cells such as platelets [3] and neurons [4] contain high levels of p60$^{c\text{-}src}$. This suggests that p60$^{c\text{-}src}$ is important in signaling in non-proliferating cells as well. However, no biological function of p60$^{c\text{-}src}$ in normal cells has been established.

Recently, Soriano et al. [5] reported that the targeted disruption of c-*src* in mice induced osteopetrosis, a disorder characterized by decreased bone resorption. Osteoclasts are multinucleated giant cells responsible for bone resorption. Kato et al. [6] reported that the osteoclasts obtained from c-*src*-disrupted mice lacked bone-resorbing activity. Almost simultaneously, Baron et al. [7] reported that rat and chick authentic osteoclasts were positively immunostained for p60$^{c\text{-}src}$. These results indicate that c-*src* is critical in osteoclastic bone resorption. We report here that p60$^{c\text{-}src}$ levels are very high, not only in authentic osteoclasts but also in osteoclast-like multinucleated cells (MNCs) formed in vitro, and that p60$^{c\text{-}src}$ is primarily localized on the ruffled border membranes of osteoclasts.

Correspondence address: T. Suda, Department of Biochemistry, School of Dentistry, Showa University, 1-5-8 Hatanodai, Shinagawa-ku, Tokyo 142, Japan. Fax: (81) (3) 3784-8555.

2. MATERIALS AND METHODS

2.1. *Materials*

Monoclonal antibody to p60$^{v\text{-}src}$ (mAb 327) was purchased from Oncogene Science Inc. (Manhassel, NY). This antibody recognizes specifically both p60$^{v\text{-}src}$ and p60$^{c\text{-}src}$, and has been used to determine the location of p60$^{c\text{-}src}$ in various primary cells and clonal cell lines [8–11]. 1α,25$(OH)_2D_3$ was purchased from Philips-Duphar (Amsterdam, The Netherlands). [^{125}I]Human calcitonin (74 TBq/mmol) was purchased from Amersham International plc (Amersham place, UK). [γ-^{32}P]ATP (111 TBq/mmol) was obtained from New England Nuclear Products (Boston, MA).

2.2. *Cells and cell cultures*

Mouse authentic osteoclasts were prepared from 1–2-day-old ddY mice (Shizuoka Laboratories Animal Center, Shizuoka, Japan) as previously described [12]. Mouse primary osteoblastic cells were obtained from 3-day-old ddy mouse calvaria. Mouse spleen cells were obtained from splenic tissues, and bone marrow cells were from tibiae of 4-week-old ddy mice as previously reported [13,14]. Osteoblastic cells (5×10^5 cells/dish) were co-cultured with spleen cells (1×10^7 cells/dish) on ø10 cm dishes (Corning; Corning, NY) in the presence of 10 nM 1α,25$(OH)_2D_3$. Mouse osteoclast-like MNCs were prepared and enriched from co-cultures of osteoblastic cells and bone marrow cells performed on 0.2% type I collagen gel-coated dishes in the presence of 1α,25$(OH)_2D_3$ according to a method previously reported [15]. Cultures were stopped at indicated times. Osteoclast-like MNCs and their precursors were identified by tartrate-resistant acid phosphatase (TRAP) staining and autoradiography using [^{125}I]human calcitonin, as previously reported [14].

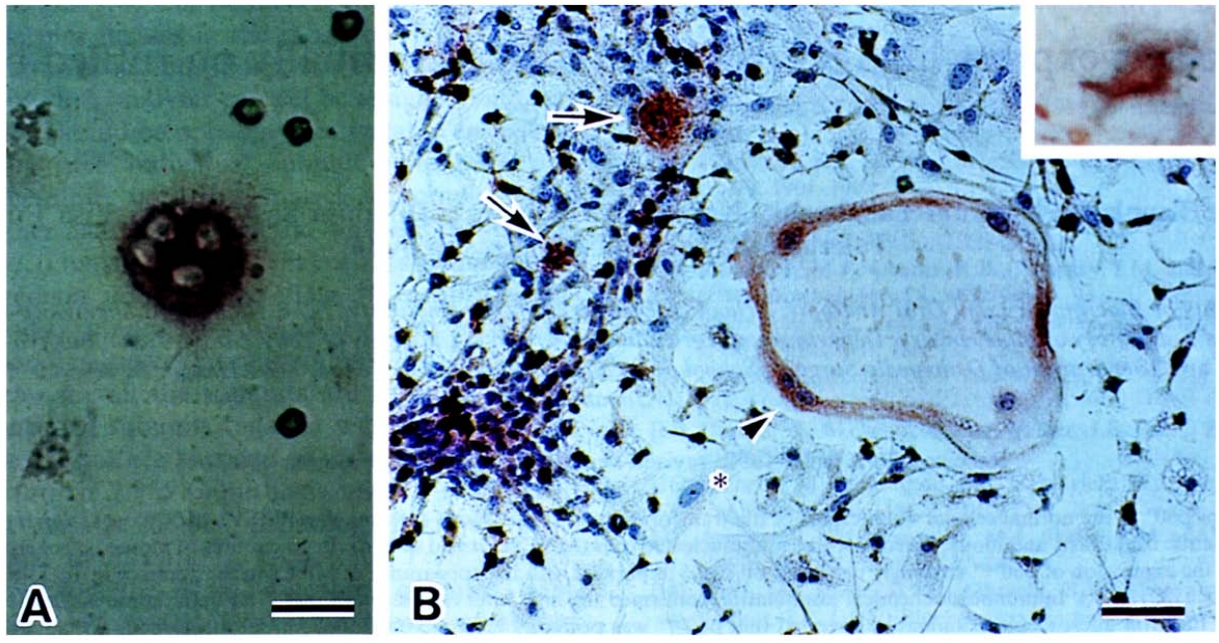

Fig. 1. Immunostaining of $p60^{c\text{-}src}$ in mouse authentic osteoclasts (A) and osteoclast-like MNCs (B, arrows) and mononuclear cells (B, arrowhead) formed in co-cultures of mouse osteoblastic cells and spleen cells in the presence of $1\alpha,25(OH)_2D_3$. Abundant [^{125}I]human calcitonin binding is evident in TRAP-positive MNCs (B, inset) and mononuclear cells (data not included) using autoradiography. Much weaker staining was observed in osteoblastic cells (B, *). Bars, 10 μm.

2.3. *Western blot analysis*

All extraction procedures were performed at 4°C. Cells were washed once with ice-cold phosphate-buffered saline (PBS), then lysed by adding 200–500 μl of cold TNE buffer (50 mM Tris-HCl (pH 7.8), 1% (v/v) Nonidet P-40, 20 mM EDTA, 2 mM sodium orthovanadate, 10 mM sodium fluoride, and aprotinin at 10 μg/ml). The supernatant was obtained by centrifugation (12,000 × g, 20 min). An equal amount (25 μg) of proteins, which were measured with a BCA protein assay kit (Pierce, Rockford, USA), were applied to 10% SDS-PAGE under a reducing condition. After electrophoresis, proteins were transferred to Immobilon-P (Millipore Corp., Bedford, MA). Immunostaining with mAb 327 was performed using ECL Western blotting detection reagents (Amersham). In short, non-specific binding was blocked by incubation with a blocking reagent overnight at 4°C. The membrane was incubated with mAb 327, then with peroxidase-linked rabbit anti-mouse immunoglobulins, and a detection reagent. Immunoblots were then visualized by exposing to X-ray films (Fuji Photo Film Co., Kanagawa, Japan).

2.4. *Immunohistochemistry*

Cultured cells were fixed with methanol/acetone (50:50, v/v) for 10 min at 4°C. Intrinsic peroxidase was blocked by incubation with 3% H_2O_2 for 15 min. Non-specific staining was blocked by incubating with a blocking agent (Histofine, Nichirei Co., Tokyo, Japan) for 1 h. Cells were incubated with mAb 327, and the bound antibody was visualized with biotinylated anti-mouse immunoglobulins, avidin–biotin-conjugated peroxidase and a DAB substrate kit (Histofine).

2.5. *Immune complex kinase assay*

The cell lysate (500 μl, 1 mg protein/ml) was incubated with 2–5 μg of mAb 327 for 1–1.5 h at 4°C and the immune complex was precipitated with protein G–Sepharose (Zymed Lab. Inc., San Francisco, CA). The immune complex was washed four times with TNE buffer and four times with kinase buffer (20 mM HEPES-NaOH, pH 7.4, and 10 mM $MgCl_2$). The immune complex was then suspended in 100 μl of reaction buffer (20 mM HEPES-NaOH (pH 7.4), 10 mM $MgCl_2$ and 40 μM ATP) with 1 μCi (37 kBq) of [γ-^{32}P]ATP in the presence of 1 μg of acid-treated enolase and incubated for 5 min at 25°C. The reaction was stopped by adding 50 μl of 3× sample buffer (187.5 mM Tris-HCl, pH 6.8, 6% SDS, 15% 2-mercaptoethanol, 30% glycerol, and 0.003% Bromophenol blue), and subjected to 10% SDS-PAGE under a reducing condition followed by autoradiography.

2.6. *Immunoelectron microscopy*

Sprague–Dawley strain rats, 4–5 weeks old, were anesthetized with an intraperitoneal injection of sodium pentobarbital and fixed by perfusion through the ascending aorta with a mixture of 4% formaldehyde and 0.1% glutaraldehyde in 0.1 M sodium cacodylate buffer (pH 7.3). After fixation, the dissected humeri were further immersed in a fresh fixative for 1–2 h at 4°C and demineralized in 10% EDTA for 2 weeks at 4°C. Their metaphyses were then washed in a 0.1 M buffer solution and embedded in medium grade LR gold resin (London Resin, Co., Basingstoke, UK). Silver–gold interference color sections were processed for immunocytochemical localization of $p60^{c\text{-}src}$ by a protein A-immunogold technique.

The sections on grids were first treated with saturated aqueous sodium metaperiodate for 30 min, followed by blocking of non-specific binding with 10% bovine serum albumin (BSA) in PBS for 30 min. They were then incubated for 2 h with mAb 327. After incubation, they were rinsed with PBS and incubated with 15 nm protein A–gold complex for 1 h. All the procedures were carried out in a moisture chamber at room temperature. After rinsing with PBS and distilled water, the sections were stained with 2% uranyl acetate and examined in a Hitachi H-800 electron microscope at 70 kV.

Semiquantification was performed from pictures. The length of membranes was measured with a Cosmosome program (Nikon, Tokyo, Japan) and the gold particles observed along the measured membrane were counted.

3. RESULTS AND DISCUSSION

Immunohistochemical analysis revealed that $p60^{c\text{-}src}$ was expressed in high levels both in authentic osteoclasts obtained from newborn mouse long bones (Fig. 1A) and in osteoclast-like MNCs formed in co-cultures

of mouse osteoblastic cells and spleen cells in the presence of $1\alpha,25(OH)_2D_3$ (Fig. 1B). In our hands, $p60^{c\text{-}src}$ showed a diffuse staining pattern which may be due to the strong fixation procedure used in this study. Otherwise, it may be due to the detection method (avidin–biotin–horseradish peroxidase method), which was suitable for demonstrating the existence of $p60^{c\text{-}src}$ but not for detecting the precise localization of the protein. Autoradiography with [^{125}I]calcitonin revealed that the osteoclast-like MNCs positively immunostained for $p60^{c\text{-}src}$ had numerous calcitonin receptors (Fig. 1B, inset). Mononuclear cells, possibly osteoclast progenitors, also expressed high levels of $p60^{c\text{-}src}$ (Fig. 1B). In contrast, osteoblastic cells showed almost negative staining (Fig. 1B). Fig. 2 shows the time-course of change in the protein levels of $p60^{c\text{-}src}$ and the number of osteoclast-like MNCs formed in co-cultures of osteoblastic cells and spleen cells in the presence of $1\alpha,25(OH)_2D_3$. The levels of $p60^{c\text{-}src}$ increased strikingly on day 5 of co-culture, and decreased by day 8 (Fig. 2B), which agreed well with the time-course of change in the number of TRAP- and calcitonin receptor-positive osteoclast-like MNCs formed in response to $1\alpha,25(OH)_3D_3$ (Fig. 2A). The level of $p60^{c\text{-}src}$ increased in neither co-cultures, which were not treated with $1\alpha,25(OH)_2D_3$, nor separate cultures of osteoblastic cells and spleen cells even in the presence of $1\alpha,25(OH)_2D_3$ (data not included). We performed immunostaining and Western blotting using another anti-*src* monoclonal antibody (GD 11), and obtained similar results (data not shown). Fig. 3 shows the phosphorylation of denatured enolase by immunoprecipitates of $p60^{c\text{-}src}$ from osteoblastic cells, co-cultures of osteoblastic cells and spleen cells, and osteoclast-like MNC-enriched fractions. The level of phosphorylation of $p60^{c\text{-}src}$ and enolase was increased in proportion to the enrichment of MNCs. These results clearly demonstrate that mouse osteoclasts and their precursors express high levels of c-*src* tyrosine kinase.

To investigate the localization of $p60^{c\text{-}src}$ in osteoclasts, we performed immunoelectron microscopy with mAb 327. Specific labeling with immunogold particles was clearly localized along the ruffled border membranes and associated pale vacuoles of osteoclasts (Fig. 3A and B). Scarce labeling was observed along the baso-

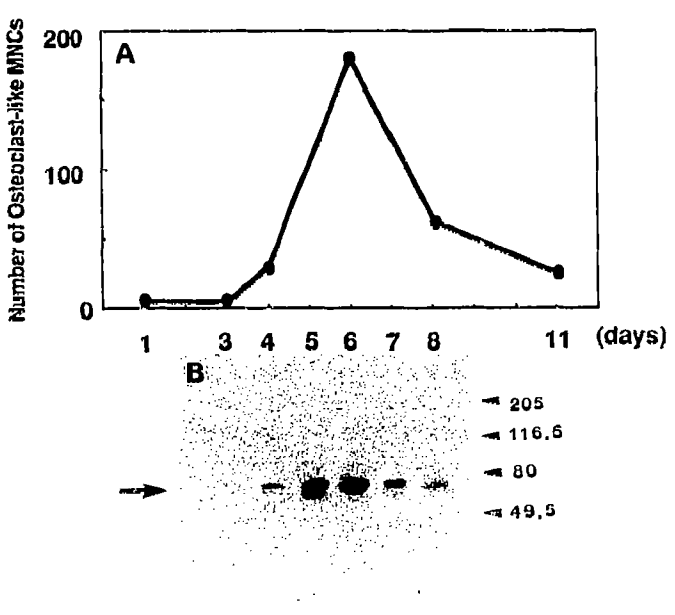

Fig. 2. Time-course of change in $p60^{c\text{-}src}$ expression (B) and the number of TRAP-positive and calcitonin receptor-positive MNCs formed in co-cultures of mouse osteoblastic cells and spleen cells (A). Osteoblastic cells and spleen cells were co-cultured in the presence of 10 nM $1\alpha,25(OH)_2D_3$, and the cultures were stopped successively on days 3, 4, 5, 6, 7 and 8. Expression of $p60^{c\text{-}src}$ was detected with Western blotting of each cell lysate (B).

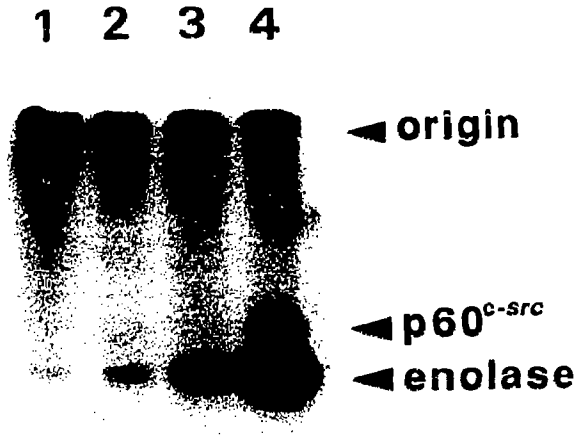

Fig. 3. Phosphorylation of acid-denatured enolase by immunoprecipitates of $p60^{c\text{-}src}$ with mAb 327. $p60^{c\text{-}src}$ was immunoprecipitated with mAb 327 from each cell lysate, and the immune complex was incubated with acid-denatured enolase in the presence of 20 μM cold ATP and 10 μCi of [γ-^{32}P]ATP. Phosphorylated enolase was detected by 10% SDS-PAGE followed by autoradiography. Lanes: 1, without immune complex; 2, osteoblastic cells; 3, co-cultures of osteoblastic cells and spleen cells; 4, osteoclast-like MNC-enriched fractions.

Table I

Semiquantification of the immunoreactivity for $p60^{c\text{-}src}$ in osteoclasts

	Number of gold particles per μm of membranes	Total length of membranes measured (μm)
Ruffled border	2.36	56.3
Clear zone	0.13	40.1
Basolateral membrane	0.18	45.6

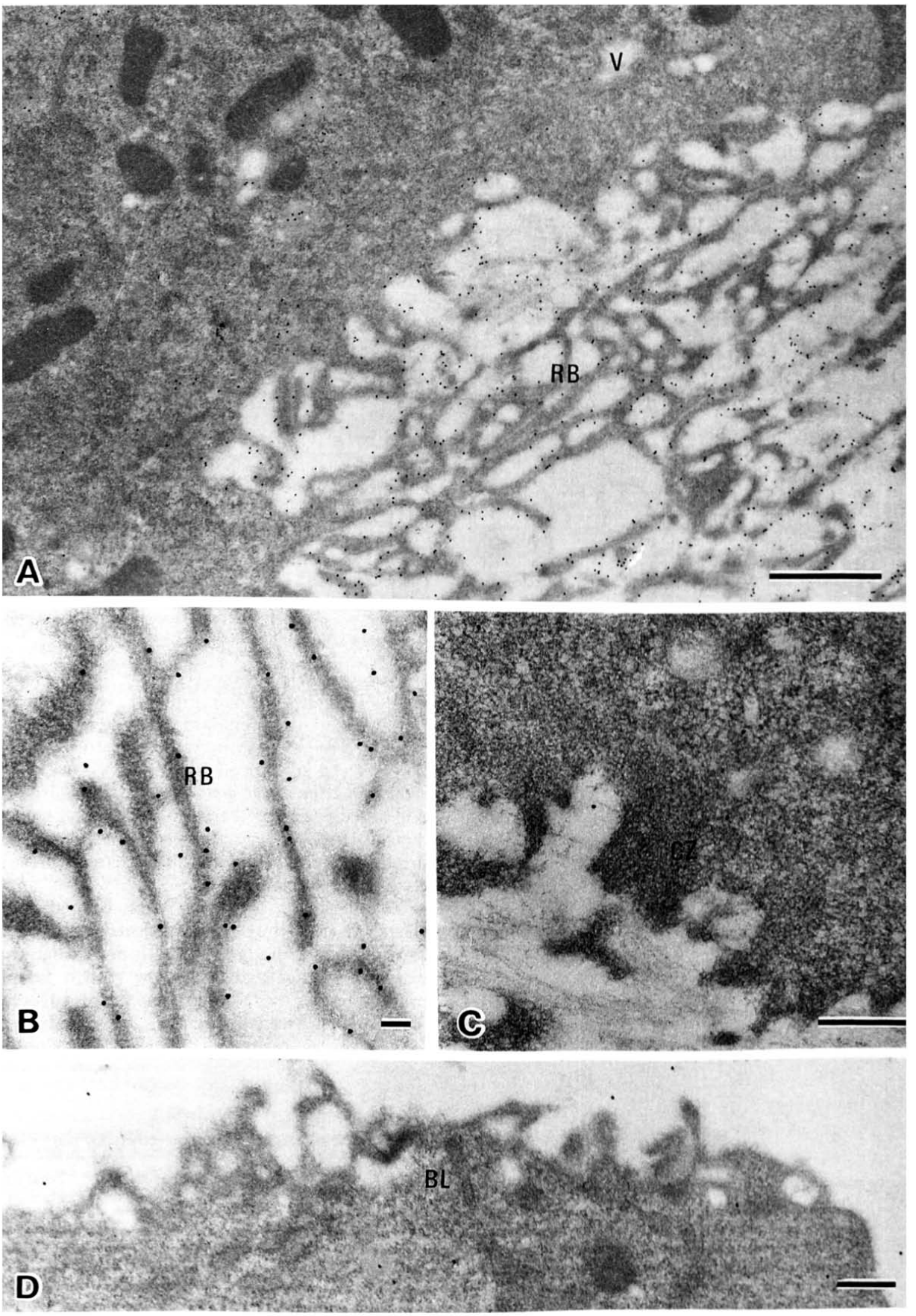
V
RB
A
RB
B
CZ
C
BL
D

lateral membranes (Fig. 3C) and clear zones (Fig. 3D). Table I shows the semiquantification of immunoreactivity of $p60^{c\text{-}src}$. The highest density of gold particles was localized on the ruffled border membrane (2.36 gold particles/μm of membrane), which was more than ten-times greater than the density on the basolateral membrane (0.18 gold particles/μm of membrane) and that on the clear zone membrane (0.13 gold particles/μm of membrane) (Table 1). The immmunoelectron microscopy was carried out using other anti-*src* monoclonal antibodies with similar results (data not shown).

Transformation of normal cells by RSV leads to change of the cell shape, in which $p60^{v\text{-}src}$ is mainly associated with the detergent-insoluble (cytoskeletal) fraction of cellular materials in RSV-transformed cells. $p60^{v\text{-}src}$ is thought to phosphorylate many cytoskeletal proteins, including vinculin, talin, ezrin, calpactin, paxillin and fibronectin receptors (reviewed in [17]). This may lead to morphological transformation of the cells by modulating such cytoskeletal proteins. Although $p60^{c\text{-}src}$ is the cellular counterpart of $p60^{v\text{-}src}$, its association with cytoskeletal proteins is much weaker than that of $p60^{v\text{-}src}$, and over-expression of $p60^{c\text{-}src}$ in normal cells does not induce cell transformation [9,18,19]. These results indicate that $p60^{c\text{-}src}$ may be involved in signal transduction pathways different from those of $p60^{v\text{-}src}$. Osteoclasts have characteristic adhesion structures called clear zones, where many actin-containing dots can be observed by fluorescence microscopy [20]. Our results clearly demonstrate that $p60^{c\text{-}src}$ is localized preferentially on ruffled border membranes and the vesicles, but not in clear zones. Moreover, we have found that phosphatidylinositol 3-kinase (PI3-kinase), which may be one of the important second messengers of $p60^{v\text{-}src}$ [21,22], has very similar distribution to $p60^{c\text{-}src}$ in rat osteoclasts (Tanaka et al., in preparation), suggesting that PI3-kinase is involved in the $p60^{c\text{-}src}$ signaling pathway. This may indicate that $p60^{c\text{-}src}$ is important for either ruffled border formation, proton secretion, or lysosomal enzyme secretion, but not for cell attachment of osteoclasts. Kato et al. [6] reported that osteoclasts from c-*src*-disrupted mice and osteoclast-like MNCs formed in bone marrow cultures from the same animals lack bone-resorbing activity. This confirms the importance of $p60^{c\text{-}src}$ in osteoclastic bone resorption, which agrees well with our finding.

In conclusion, osteoclast-like MNCs formed in our co-culture system express high levels of $p60^{c\text{-}src}$, and provide a suitable model for investigating the role of $p60^{c\text{-}src}$ in normal cells.

REFERENCES

[1] Jove, R. and Hanafusa, H. (1987) Annu. Rev. Cell Biol. 3, 31–56.
[2] Golden, A. and Brugge, J.S. (1988) in: The Oncogene Handbook (Reddy, E.P., Skalka, A.M. and Curran, T. eds.) Elsevier, Amsterdam.
[3] Brugge, J.S., Cotton, P.C., Queral, A.E., Barret, J., Nonner, D. and Keane, R. (1985) Nature 316, 524–526.
[4] Golden, A., Nemeth, S.P. and Brugge, J.S. (1986) Proc. Natl. Acad. Sci. USA 83, 852–856.
[5] Soriano, P., Montgonery, C., Geske, R. and Bradley, A. (1991) Cell 64, 693–702.
[6] Kato, I., Yoneda, T., Izbicka, E., Lee, C., Gutierrez, G., Boyce, B., Soriano, P. and Mundy, G.R. (1991) J. Bone Min. Res. 6, S197.
[7] Baron, R., Chatteriee, D., Horne, W., Levy, J., Lomri, A. and Neff, L. (1991) J. Bone Min. Res. 6, S197.
[8] Lipsich, L.A., Lewis, A.J. and Brugge, J.S. (1983) J. Virol. 48, 352–360.
[9] Shalloway, D., Coussens, P.M. and Yaciuk, P. (1984) Proc. Natl. Acad. Sci. USA 81, 7071–7075.
[10] David-Pfeuty, T. and Nouvian-Dooghe, Y. (1990) J. Cell Biol. 111, 3097–3116.
[11] Linstedt, A.D., Vetterm, M.L., Bishop, J.M. and Kelly, R.B. (1992) J. Cell Biol. 117, 1077–1084.
[12] Chambers, T.J. and Magnus, C.J. (1982) J. Pathol. 136, 27–40.
[13] Takahashi, N., Yamana, H., Yoshiki, S., Roodman, G.D., Mundy, G.R., Jones, S.J., Boyde, A. and Suda, T. (1988) Endocrinology 122, 1373–1382.
[14] Takahashi, N., Akatsu, T., Udagawa, N., Sasaki, T., Yamaguchi, A., Mosley, J.M., Martin, T.J. and Suda, T. (1988) Endocrinology 123, 2600–2602.
[15] Akatsu, T., Tamura, T., Takahashi, N., Udagawa, N., Tanaka, S., Sasaki, T., Yamaguchi, A., Nagata, N. and Suda, T. (1992) J. Bone Miner. Res. (in press).
[16] Hamaguchi, M. and Hanafusa, H. (1987) Proc. Natl. Acad. Sci. USA 84, 2312–2316.
[17] Burridge, K., Fath, K., Kelly, T., Nuckolls, G. and Turner, C. (1988) Annu. Rev. Cell. Biol. 4, 487–525.
[18] Parker, R.C., Varmus, H.E. and Bishop, J.M. (1984) Cell 37, 131–139.
[19] Iba, H., Takeya, T., Cross, F.R. and Hanafusa, H. (1984) Proc. Natl. Acad. Sci. USA 81, 4424–4428.
[20] Marchishio, P.C., Cirillo, D., Naldini, L., Primavera, M.V. and Zambonin-Zallone, A. (1984) J. Cell Biol. 99, 1696–1705.
[21] Fukui, Y. and Hanafusa, H. (1989) Mol. Cell. Biol. 9, 1651–1658.
[22] Fukui, Y., Kornbluth, S., Jong, S.-M., Wang, L.-H. and Hanafusa, H. (1989) Oncogene Res. 4, 283–292.

←

Fig. 4. Immunoelectron micrographic localization of $p60^{c\text{-}src}$ in rat authentic osteoclasts with mAb 327. Heavy immunolabeling was observed along ruffled border membranes (A and B, **RB**) and associated pale vacuoles (A, **V**). Only a few gold particles were seen at the clear zone region (C, **CZ**) and the basolateral membranes (D, **BL**). Bars: A, 1 μm; B, 100 nm; C, 1 μm; and D, 1 μm.